Assessing Risk from Cascading Blackouts Given Correlated Component Failures

Laurence A. Clarfeld, Margaret J. Eppstein, Paul D.H. Hines and Eric M. Hernandez
University of Vermont, Burlington, VT, USA

***Abstract*—Despite the infrequent occurrence of cascading power failures, their large sizes and enormous social costs mean that they contribute substantially to the overall risk to society from power failures in the grid. Therefore it is important to accurately understand the risk associated with such events. A cascading event may be triggered by a small subset of k components failing simultaneously or in rapid succession. While most prior work, including our own work into an efficient "Random Chemistry" method for risk analysis, has assumed that components fail independently, this paper proposes a method for deriving correlated outage probabilities such that pairs of branches that are proximate in space are more likely to fail together than distant ones. Combining Random Chemistry risk analysis with this approach to correlated outage probabilities shows that overall blackout risk can greatly increase with even small amounts of correlation. Results from the 2383-bus Polish test case under various load levels illustrate the substantial impact that correlation has on blackout risk.**

***Index Terms*—blackout risk, cascading failure, cascading outage, correlated outages, Random Chemistry**

I. Introduction

A cascading power failure occurs when a small number of components in a power grid fail, setting off a chain reaction of subsequent component failures that can lead to large blackouts. Cascading power failures are rare events, but their vast size means they pose a significant risk to power grids [1]–[3]. Reliability regulations require that power systems be operated to be robust to single component failures ($N-1$ security) and increasingly require that grid operators make plans to ensure $N-k$ security [4]. There is, however, no guarantee that sets of two or more components failing together will not cause a cascade. Sets of k simultaneous outages are typically referred to as $N-k$ contingencies. Furthermore, mechanisms such as "hidden failures" can exacerbate the risk and impact of cascades [5]–[7]. In this paper, we consider only branch outages. We refer to sets of k branch outages that initiate a cascading failure as $N-k$ malignancies whereas sets of k branch outages that do not cause a cascade are referred to as benign contingencies.

The combinatorial search space of $N-k$ contingencies makes it difficult to estimate risk in a computationally tractable manner. A number of existing papers propose methods for quantifying the risk of cascading failure [8]–[13]. A limitation of most prior approaches (including our own) is the assumption that branch outages are independent events [1], [11], [12], [14], [15].

In reality, branch failures are unlikely to be independent when a common cause is responsible for the outages. For example, damage caused by weather-related disturbances may be spatially correlated [16]. Protection system failures can sometimes cause multiple outages within a small geographic region [17]. Similarly, terrorist attacks may be spatially localized. This type of geographical correlation was handled in [18] by assuming 100% correlation of outages within a fixed radius. In [16] spatial correlation was achieved by probabilistically determining failure rates of lines adjacent to initial failures according to a Poisson process. In [19], a random field with spatial autocorrelation was used in a cascade model to assess risk from common-cause events. Correlation between outages can also be associated with non-spatial attributes such as component age [20].

Another way to correlate component failures is though copula analysis. Copulas have been applied in many fields, such as finance [21], neuroscience [22], and climate research [23]. Within the realm of power systems, copulas are a popular tool for uncertainty analysis, such as in [24]. In [25], Li suggests copulas as a useful way to incorporate correlation between random variables in power systems risk analysis. Here, we will present the use of a Gaussian copula and show that incorporating even modest levels of correlation can greatly increase the risk associated with cascading failures.

A. Finding Triggering Events with "Random Chemistry"

In [26] we introduced an efficient ($O(\log N)$) stochastic set size reduction algorithm referred to as "Random Chemistry" (RC) for identifying small minimal sets of initiating events that trigger some outcome of interest. In [27] we applied RC to the problem of identifying minimal $N-k$ malignancies that lead to cascading failures in power grids (Fig. 1), where N is the total number of branches in the power system. In [11], [12], [15] we showed that RC can be used to efficiently estimate the system-wide risk of large cascading failures in power grids. A comparison of risk estimation to Monte Carlo (MC)

This work was supported in part by the US National Science Foundation, award Nos. ECCS-1254549 and IGERT: Smart Grids - Technology, Human Behavior and Policy (NSF Award #DGE-1144388).
L. Clarfeld and M. Eppstein are with the Dept. of Computer Science, U. of Vermont, 05408, e-mails: Laurence.Clarfeld@uvm.edu, Maggie.Eppstein@uvm.edu.
P. Hines is with the Dept. of Electrical and Biomedical Engineering, U. of Vermont, 05408, e-mail: Paul.Hines@uvm.edu.
E. Hernandez is with the Dept. of Civil and Env. Engineering, U. of Vermont, 05408, e-mail: Eric.Hernandez@uvm.edu.

simulation on a model of the Polish system at peak winter load [28] showed that the RC approach is at least two orders of magnitude faster than MC, and does not introduce measurable bias into the estimate [12], [15]. Simulations were conducted using DCSIMSEP, a simulator of cascading outages leading to network separation in power systems [29]. We found that a small number of branches disproportionately affect overall risk. In these previous works we assumed uncorrelated branch outages; here, we relax that assumption and generalize this approach to systems with correlated outages.

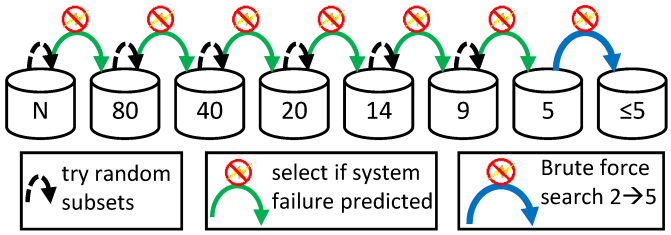

Figure 1. Schematic of the RC algorithm applied to finding a minimal $N-k$ malignancy in a power system (abstracted from [27]).

B. Estimating Risk

For any given set of branches ω that cause a cascading failure, risk can be calculated as:

$$R_\omega = p_\omega s_\omega \tag{1}$$

where p_ω is the joint probability of the branches in ω failing and s_ω is the size of the resultant blackout. Note that p_ω is itself a function of p_i, the independent outage probability for each branch i, and any effect of correlation among branch outage probabilities. In this paper, s_ω is quantified as the total power (MW) unserved due to load shedding. The total risk posed to the system by $N-k$ malignancies, for a given k, is then:

$$R_k = \sum_{\omega \in \Omega_k} R_\omega \tag{2}$$

where Ω_k is the complete set of all $N-k$ malignancies for each $k \geq 2$. The overall risk R of cascading failure due to all $k \leq k_{max}$ is thus:

$$R = \sum_{k \in \{2..k_{max}\}} R_k \tag{3}$$

The RC (or any other) algorithm is unlikely to find the entire set Ω_k for $k > 2$ on realistically sized systems, because of the computationally intractable sizes of these sets. However, various approaches have been used to estimate the number of $N-3$ malignancies $|\Omega_3|$ from changes in the rate of identification of new unique $N-3$ malignancies. This can then be used to project system risk for $k_{max} = 3$ from the identified sets of $N-2$ and $N-3$ malignancies [15], [27].

II. Copula Analysis

Nelsen [30] defines copulas as "functions that join or couple multivariate distribution functions to their one-dimensional marginal distribution functions". Given a set of k random variables, $\mathbf{X} = [X_1, X_2, \ldots, X_k]$, where $\Pr(X_i \leq t_i)$ is the marginal probability that branch i fails, for some threshold t_i, then

$$F_X(\mathbf{T}) = \Pr\left(\bigcap_{i=1}^{k} X_i \leq t_i\right) \tag{4}$$

where $\mathbf{T} = [t_1, t_2, \cdots, t_k]$, represents the joint probability that all k branches fail together. Without loss of generality, we assume that $t_i = 0$ for all i. There are numerous classes of copula functions in popular use. For this proof-of-concept study, we assume a Gaussian copula. Alternative distributions may be assumed where appropriate.

We make the application to branch outages by assuming that the (inverse) stress on a line i is a univariate Gaussian random variable $X_i = \mathcal{N}(\mu_i, \sigma_i)$ with the cumulative distribution function:

$$F_{X_i}(x_i) = \frac{1}{2}\left[1 + \text{erf}\left(\frac{x_i - \mu_i}{\sigma_i\sqrt{2}}\right)\right] \tag{5}$$

Given that the independent probability of branch i failing is p_i, we can choose μ_i and σ_i such that when X_i goes below zero, the branch fails. In other words, we choose μ_i and σ_i such that $F_{x_i}(0) = p_i$ for each branch i. Without loss of generality, we can assume $\mu_i = 1$ for all i and then solve for each σ_i, as follows:

$$\sigma_i = \frac{-1}{\text{erf}^{-1}(2p_i - 1)\sqrt{2}} \tag{6}$$

Now that we have constructed the univariate marginal distributions for each branch, we can use a multivariate normal distribution $\mathbf{X} = \mathcal{N}(\boldsymbol{\mu}, \mathbf{C})$ with mean $\boldsymbol{\mu} = [\mu_1, \mu_2, \ldots, \mu_k]$ and covariance matrix $\mathbf{C}$ as our copula function (Fig. 2).

In this study, we assume the correlation between failures in branches i and j decays exponentially with the distance between them d_{ij}, according to:

$$\rho_{ij} = \rho_o e^{-d_{ij}/L} \tag{7}$$

where ρ_o represents the maximum possible correlation coefficient (at distance zero) and L represents the characteristic length, which controls the decay rate of the correlation. L can be interpreted as the distance at which ρ_{ij} reaches $e^{-1} \approx 36.8\%$ of ρ_o (Fig. 3).

The parameters ρ_o and L can be used to tune the strength of the correlation as desired. We use the standard deviations σ_i and σ_j calculated by (6) and the correlation coefficient ρ_{ij} calculated by (7) to calculate the pairwise covariance between branches i and j as:

$$\text{cov}(i,j) = \rho_{ij}\sigma_i\sigma_j \tag{8}$$

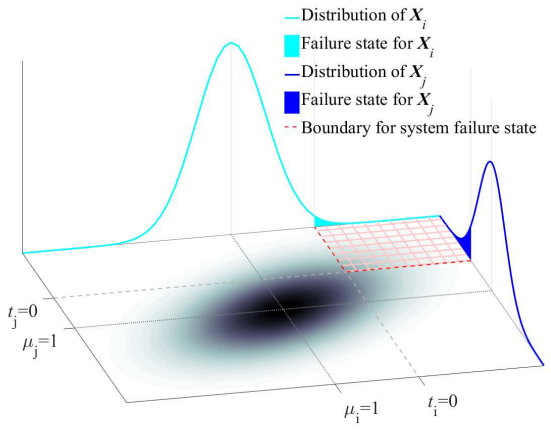

Figure 2. A visual depiction of the copula method for two components with hypothetical Gaussian distributions, X_i and X_j. The curves on the vertical planes represent the marginal distributions of each component, with the shaded regions of these curves, $(X_i \leq 0)$ and $(X_j \leq 0)$, representing the failure state for each component. The shaded gradient on the horizontal plane represents the density of the joint distribution (copula) of the two variables, with darker shading representing higher density. The probability mass within the red hatched area represents the region of system failure ($\mathbf{X} \leq 0$), with the red dotted line depicting the boundaries of this region.

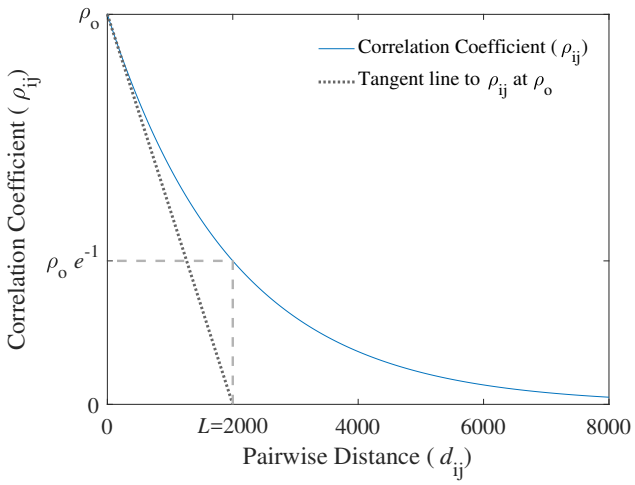

Figure 3. Change in the correlation between two branches as a function of the distance between them, assuming (7) with characteristic length $L = 2000$ and correlation ρ_o for branches that are 0 units of distance apart.

Using (8) to find each element of the covariance matrix $\mathbf{C}$, we can then use the probability density function of the multivariate normal distribution (9) to form our copula.

$$f(\mathbf{x}) = \frac{1}{\sqrt{(2\pi)^k |\mathbf{C}|}} \exp\left\{-\frac{1}{2}(\mathbf{x}-\boldsymbol{\mu})^\top \mathbf{C}^{-1}(\mathbf{x}-\boldsymbol{\mu})\right\} \quad (9)$$

Using our copula function, $F_X(\mathbf{0})$ will represent the joint probability of system failure $\Pr(\mathbf{X} \leq \mathbf{0})$, when all k components fail together. To calculate $F_X(\mathbf{0})$ we integrate over the region in the joint distribution that represents failure of all system components.

$$F_X(\mathbf{x}) = \int_{-\infty}^{0}\int_{-\infty}^{0}\cdots\int_{-\infty}^{0} f(x_1, x_2, \ldots, x_k)\,\mathrm{d}x_1\,\mathrm{d}x_2\ldots\,\mathrm{d}x_k \quad (10)$$

The multiple-integral in (10) represents the generalized solution for arbitrary k. In this work, we consider only $k = 2$ and solve the resultant double-integral numerically using the vectorized adaptive quadrature method [31].

III. Case Study

We extend our previous work assessing cascading failure risk [11], [12], which also used the Polish test case at peak winter load [28], to account for spatially correlated outages. As previously noted, in this proof-of-concept study we only consider $N-2$ malignancies and assume Gaussian copulas. However, the approach is readily generalizable to greater values of k (assuming $|\Omega_k|$ can be estimated) and/or alternative distribution functions.

Simulations were conducted using the 2383-bus, 2896-branch Polish power system, at the 1999 peak winter load, which is available via the MATPOWER simulation package [28]. As described in [11], [12], we made several modifications to this test case, including an increase in line limits by a factor of 1.05 above the pre-contingency line flows that occur when the system is at 1.10 times actual load. This change was made to ensure that this "base case" is $N-1$ secure. We then examined loads that were 55% to 115% of the base case, to assess how risk changes under varying load conditions.

The true spatial locations of branches and buses are not publicly available for this test case, so hypothetical locations were inferred based on a graph layout of the grid topology, assuming branches are straight lines between buses (Fig. 4).

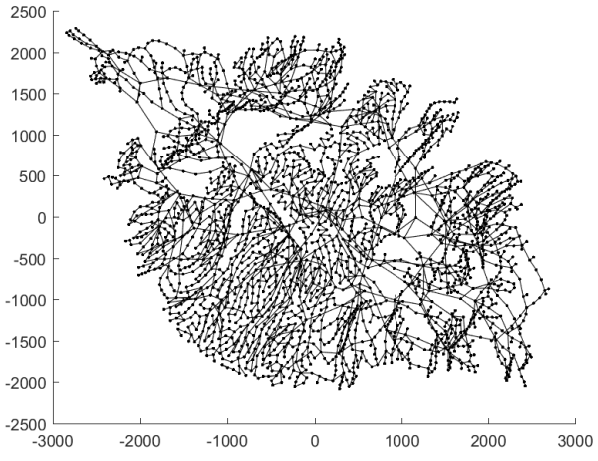

Figure 4. Synthetic geographic layout of the Polish test case (in arbitrary units).

Since the network topography used is thus artificial, all distances are considered to have "arbitrary units". Additionally,

as described in [11], [12], we assigned branch failure rates randomly from a normal distribution with the same mean and variance as those provided by the RTS-96 test case [32], since these rates were unavailable for the Polish grid.

A. Distance Metric

The appropriate definition of "distance" may vary depending on the type of common cause threating the system. Without loss of generality, we employ a proximity-based metric that assumes branches are straight lines. Consider branches U with endpoints (u_1, u_2) and V with endpoints (v_1, v_2). Let the distance from U to V be defined as

$$\mathrm{Dist}(U,V) = \frac{\sum_{i=1}^{2} d(u_i, V) + \sum_{i=1}^{2} d(v_i, U)}{2} \qquad (11)$$

where $d(u_i, V)$ is the minimum euclidean distance from the point u_i to the line segment $V = (v_1, v_2)$, as illustrated in Fig. 5.

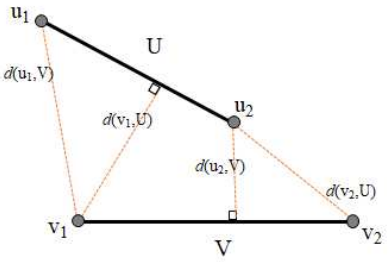

Figure 5. Visual example for calculating the distance between branches U and V with endpoints (u_1, u_2) and (v_1, v_2), respectively.

In this formulation, it is worth noting that $d(u_i, V) \neq d(v_i, U)$. This makes sense when considering branches of different lengths. For example, consider branches A and B in Fig. 6. All of B's span overlaps with A while only a portion of A's span overlaps with B, so it follows that B is in some sense closer to A than A is to B. This asymmetry is handled by averaging $d(u_i, V)$ and $d(v_i, U)$ in (11). This distance metric conforms with what would be intuitively expected when considering spatially correlated damage, as seen in Fig. 6, where $\mathrm{Dist}(A, B) > \mathrm{Dist}(C, D)$ and $\mathrm{Dist}(E, F) > \mathrm{Dist}(G, H)$.

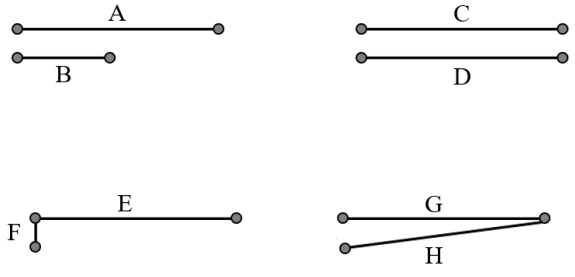

Figure 6. Branch pairs used for pairwise distance examples described in the text.

Using this metric, a pair of branches will have distance 0 only if they are parallel branches between the same buses. This definition of distance can be extended to larger subsets of branches by taking the average of the pairwise distances:

$$\mathrm{Dist}(U_1, U_2, \ldots, U_k) = \frac{2\sum_{i=1}^{k-1}\sum_{j=i+1}^{k} \mathrm{Dist}(U_i, U_j)}{k(k-1)} \qquad (12)$$

The distribution of pairwise branch distances in the 2896-branch Polish grid, according to (11) and assuming the topography shown in Fig. 4, is shown in Fig. 7. Branch pairs that cause cascading failures are relatively rare, with only 0.013% of branch pairs comprising $N-2$ malignancies. While there is a significant relationship between branch distance and blackout size ($\mathrm{p} < 0.01$), the amount of difference explained by branch distance is very low ($\mathrm{R}^2 = 0.019$). However malignant pairs tend to be much closer to each other than benign pairs (Fig. 8), as supported by a two-sample Kolmogorov-Smirnov test on the two distributions ($\mathrm{p} \ll 0.01$). This tendency for branch pairs in $N-2$ malignancies to be close together will exacerbate the impact of spatial correlation to our cascading failure risk calculations.

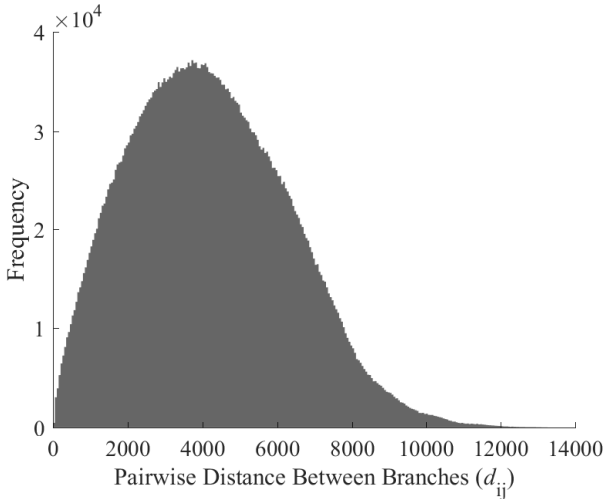

Figure 7. Distribution of pairwise branch distances in the Polish grid using the proposed proximity-based distance method, in arbitrary units.

B. Results

The total system risk contributed by $N-2$ malignancies was calculated for spatially correlated branch outages across a range of scenarios. Risk was calculated for varying load levels from 55%-115% of 2004 peak winter load in the adjusted Polish grid, for all combinations of $L \in \{0, 500, 1000, 1500, 2000\}$ and $\rho_o \in \{0, 0.05, 0.10, 0.15\}$.

Changes in the total system risk as a function of load at $L = 2000$ (the longest characteristic correlation length tested), over the different values tested for ρ_o, are shown in Fig. 9. As noted in [12], risk varies non-monotonically with load, in part due to variations in the proximity of generation to demand that result from optimal power flow dispatch at different load levels. With this characteristic length, even at $\rho_o = 0.05$, risk in the correlated case from load levels 98%-111% surpass the maximum risk seen in the uncorrelated case at any load

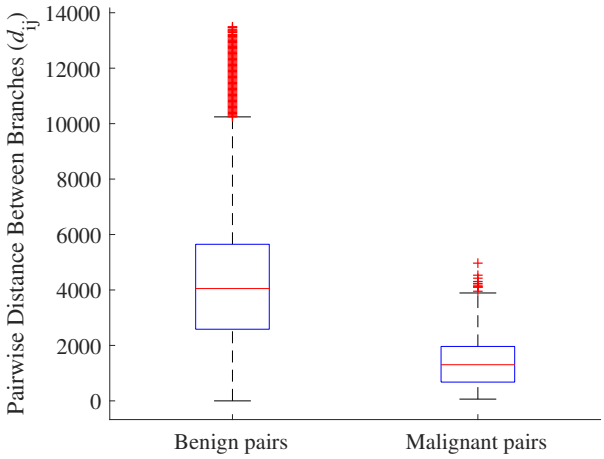

Figure 8. Comparison of distance between branches pairs that form $N-2$ malignancies vs. benign pairs that do not lead to cascading failure, using the proposed proximity-based distance metric from (11). The horizontal red line on the boxplot represents the median, the top and bottom of the blue box represent the 25th and 75th quartiles, respectively, and the red "+" signs are outliers.

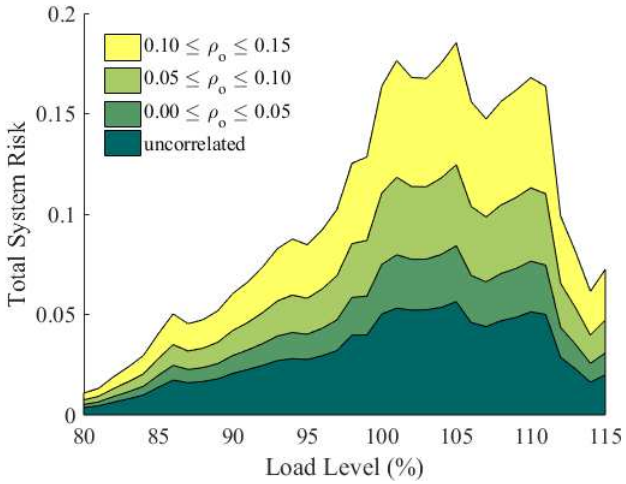

Figure 9. Overall system risk posed by spatially-correlated $N-2$ malignancies with a characteristic correlation length of $L = 2000$ and various values of maximum correlation ρ_o, at load levels that are 80%-115% of the 2004 Polish peak winter load.

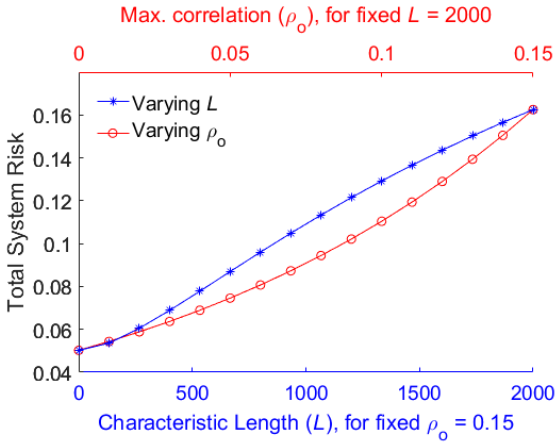

Figure 10. Comparing change in total system risk for varying L (ρ_o fixed at 0.15) vs. varying ρ_o (L fixed at 2000) for the 100% load level of the 2004 Polish peak winter load

level tested (up to 115%). The highest overall system risk found occurred at 105% load with $L = 2000$ and $\rho_o = 0.15$, where risk increased 225% over the uncorrelated estimate. The greatest relative increase in risk, as a function of ρ_o, occurred at the lowest load levels, where overall system risk was lowest. However, the greatest absolute increases in risk, as a function of ρ_o, occurred at load levels of 95%-112%, where there were the most $N-2$ malignancies. For a given load level, risk increases faster than linearly as ρ_o increases (Fig. 10).

Just as ρ_o can influence risk, so too can the characteristic length (L), as shown in Fig. 11. Results are included from load levels 80%-115% for $\rho_o = 0.15$. As expected, increasing L for a given ρ_o increases risk. However, in this case the rate of increase is non-monotonic, with the largest increases at intermediate values of L (Fig. 10), because the effect of increasing L diminishes as L approaches the diameter of the grid topography.

It is also informative to investigate the degree to which each branch contributes to overall risk as a function of spatial correlation. Given branch i with independent outage probability of p_i, we can measure i's contribution to total risk posed by $N-k$ malignancies by finding the sensitivity, $S_k(i)$ of risk to p_i. As discussed in [11], [12], this equates to a partial derivative of risk with respect to p_i. Here, we estimate these sensitivities using a finite difference approximation:

$$S_k(i) = \frac{\partial R_k(p_i)}{\partial p_i} \approx \frac{R_k(p_i + \Delta p_i) - R_k(p_i)}{\Delta p_i} \qquad (13)$$

where $R_k(p_i + \Delta p_i)$ is the total risk of the system posed by $N-k$ malignancies when p_i is increased by a small amount Δp_i. In our calculations, we used $\Delta p_i = 10^{-15}$; empirical tests showed that further decreasing Δp_i did not substantially change the results. Branch sensitivities were calculated at the 100% load level with $\rho_o = 0.15$ and $L = 500$. Branch sensitivities in the correlated case described above are approximately 1.4 times that of the uncorrelated case (Fig. 12). The overall relative order of branch sensitivity is largely, but not entirely, preserved (Spearman's rank correlation $r_s = 0.947$). For example, if we look just at the ten most sensitive branches (i.e., those of greatest concern) there are notable changes in the relative ordering of branch sensitivity between the uncorrelated and correlated case ($r_s = 0.758$).

IV. Discussion

A number of recent papers on cascading failure risk assume that branch outages are statistically independent events. This assumption neglects the possibility of common cause failures such as relay failures, weather events, or terrorist attacks. This paper presents a systematic method to account for spatial correlations among branch outages. The copula-based method

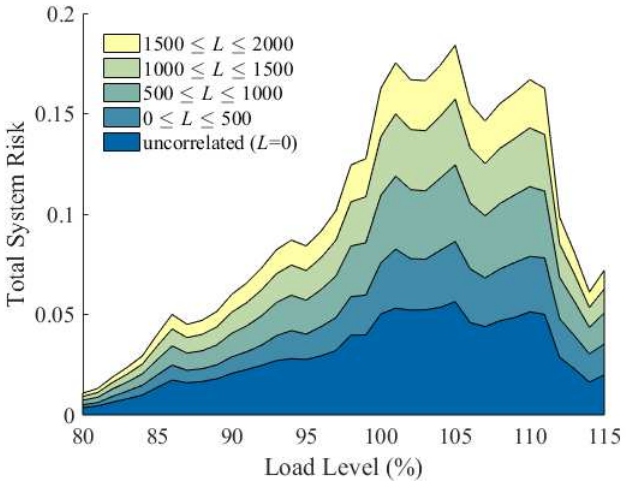

Figure 11. Overall system risk posed by spatially-correlated $N-2$ malignancies with a maximum correlation coefficient of $\rho_o = 0.15$ and various values of characteristic correlation length L, at load levels that are 80%-115% of the 2004 Polish peak winter load.

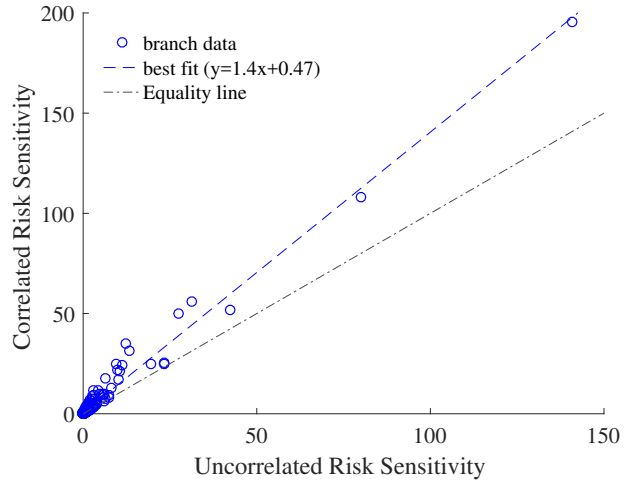

Figure 12. Comparison of branch sensitivities for each branch in uncorrelated ($L = 0$) vs. correlated ($L = 500$) risk estimates associated with $N - 2$ malignancies in the Polish Grid at 2004 peak winter load, and with $\rho_o = 0.15$.

described and demonstrated here is general in that it can be tailored to the details of a specific power system and disturbance category. Parametric choices include the correlation function and associated constants, the distance metric, and the distribution of the copula function.

The application of the method to a large power systems test case shows that even small correlations between component failures can lead to significant increases in system risk posed by $N-2$ malignancies. This increase in risk is exacerbated by the fact that branch pairs that are close together in this system are more likely to cause cascading failures than are branch pairs that are farther apart.

Prior studies have shown that, in the spatially uncorrelated case, the sensitivity of risk to individual branch outages exhibits a very heavy-tailed distribution, with a few branches contributing disproportionately to risk [12]. Adding spatial correlation to branch outages magnifies this disparity in the relative contributions of each branch to the overall system risk. Futhermore, the relative sensitivity of risk to different branch outages can differ between the uncorrelated and correlated cases, especially in the branches with the highest sensitivities. These observations may have important implications for proposed strategies to mitigate risk by reducing the flow on the most sensitive branches [11].

The results presented in this paper suggest that practical approaches to $N - k$ cascading failure risk is possible. Reliability regulations (e.g., NERC TOP-004-1.R3) increasingly require that transmission system operators study and protect their systems against the risk of cascading failures triggered by $N - k$ outages. The method presented here has sufficient computational efficiency to be useful in operations planning tools that quantify the risk of $N-k$ events and quickly identify important sources of that risk. A key element needed to make this sort of tool practical is better data about the probability of transmission branch outages and the ways in which different types of common causes impact those probabilities. Some data that would be helpful for tuning this model are available to industry through systems such as the NERC TADS database, but these data are not typically available for research.

Future work will study the impact of parametric choices and design details on risk in a variety of test cases, including those with more accurate geographical data (e.g., [33]), and will apply a more sophisticated AC cascading failure simulator. In addition, we will extend this work to analyze spatially correlated $N - k$ malignancies for $k > 2$. This will yield insights as to whether spatial correlation increases or decreases the relative importance of higher-order $N - k$ malignacies on risk, with important practical implications for methods designed to estimate the risk of cascading failures.

REFERENCES

[1] Q. Chen, C. Jiang, W. Qiu, and J. D. McCalley, "Probability models for estimating the probabilities of cascading outages in high-voltage transmission network," *IEEE Transactions on Power Systems*, vol. 21, no. 3, pp. 1423–1431, Aug. 2006.

[2] I. Dobson, B. A. Carreras, V. E. Lynch, and D. E. Newman, "Complex systems analysis of series of blackouts: Cascading failure, critical points, and self-organization," *Chaos: An Interdisciplinary Journal of Nonlinear Science*, vol. 17, no. 2, p. 026103, Jun. 2007.

[3] D. P. Nedic, I. Dobson, D. S. Kirschen, B. A. Carreras, and V. E. Lynch, "Criticality in a cascading failure blackout model," *International Journal of Electrical Power & Energy Systems*, vol. 28, no. 9, pp. 627–633, Nov. 2006.

[4] S. NERC, "Top-004–2: Transmission operations," *North American Electric Reliability Corporation*, 2007.

[5] J. Chen, J. S. Thorp, and I. Dobson, "Cascading dynamics and mitigation assessment in power system disturbances via a hidden failure model," *International Journal of Electrical Power & Energy Systems*, vol. 27, no. 4, pp. 318–326, 2005.

[6] X. Yu and C. Singh, "A practical approach for integrated power system vulnerability analysis with protection failures," *IEEE Transactions on Power Systems*, vol. 19, no. 4, pp. 1811–1820, 2004.

[7] D. C. Elizondo, J. de La Ree, A. G. Phadke, and S. Horowitz, "Hidden failures in protection systems and their impact on wide-area disturbances," in *Power Engineering Society Winter Meeting, 2001. IEEE*, vol. 2. IEEE, 2001, pp. 710–714.

[8] I. Dobson, K. R. Wierzbicki, J. Kim, and H. Ren, "Towards quantifying cascading blackout risk," in *Bulk Power System Dynamics and Control-VII. Revitalizing Operational Reliability, 2007 iREP Symposium*. IEEE, 2007, pp. 1–12.

[9] M. Vaiman, K. Bell, Y. Chen, B. Chowdhury, I. Dobson, P. Hines, M. Papic, S. Miller, and P. Zhang, "Risk assessment of cascading outages: Methodologies and challenges," *IEEE Transactions on Power Systems*, vol. 27, no. 2, p. 631, 2012.

[10] Q. Chen and L. Mili, "Composite power system vulnerability evaluation to cascading failures using importance sampling and antithetic variates," *Power Systems, IEEE Transactions on*, vol. 28, no. 3, pp. 2321–2330, Aug 2013.

[11] P. Rezaei, M. J. Eppstein, and P. D. H. Hines, "Rapid Assessment, Visualization, and Mitigation of Cascading Failure Risk in Power Systems," in *2015 48th Hawaii International Conference on System Sciences*, Jan. 2015, pp. 2748–2758.

[12] P. Rezaei, P. D. Hines, and M. J. Eppstein, "Estimating cascading failure risk with random chemistry," *IEEE Transactions on Power Systems*, vol. 30, no. 5, pp. 2726–2735, 2015.

[13] P. D. Hines, I. Dobson, and P. Rezaei, "Cascading power outages propagate locally in an influence graph that is not the actual grid topology," *IEEE Transactions on Power Systems*, vol. 32, no. 2, pp. 958–967, 2017.

[14] K. Kck, H. Renner, and J. Stadler, "Probabilistic cascading event risk assessment," in *2014 Power Systems Computation Conference*, Aug. 2014, pp. 1–7.

[15] P. Rezaei, P. D. H. Hines, and M. Eppstein, "Estimating cascading failure risk: Comparing Monte Carlo sampling and Random Chemistry," in *2014 IEEE PES General Meeting | Conference Exposition*, Jul. 2014, pp. 1–5.

[16] I. Dobson, N. Carrington, K. Zhou, Z. Wang, B. Carreras, and J. Reynolds-Barredos, "Exploring Cascading Outages and Weather via Processing Historic Data," in *Proc. 51st Hawaii International Conference on System Sciences*, 2018.

[17] K. Jiang and C. Singh, "New models and concepts for power system reliability evaluation including protection system failures," *IEEE Transactions on Power Systems*, vol. 26, no. 4, pp. 1845–1855, 2011.

[18] A. Bernstein, D. Bienstock, D. Hay, M. Uzunoglu, and G. Zussman, "Power grid vulnerability to geographically correlated failuresanalysis and control implications," in *INFOCOM, 2014 Proceedings IEEE*. IEEE, 2014, pp. 2634–2642.

[19] A. Scherb, L. Garr, and D. Straub, "Reliability and Component Importance in Networks Subject to Spatially Distributed Hazards Followed by Cascading Failures," *ASCE-ASME Journal of Risk and Uncertainty in Engineering Systems, Part B: Mechanical Engineering*, vol. 3, no. 2, pp. 021 007–021 007–9, Mar. 2017.

[20] W. Li, "Incorporating aging failures in power system reliability evaluation," *IEEE Transactions on Power Systems*, vol. 17, no. 3, pp. 918–923, Aug 2002.

[21] U. Cherubini, E. Luciano, and W. Vecchiato, *Copula Methods in Finance*. John Wiley & Sons, Oct. 2004.

[22] A. Onken, S. Grnewlder, M. H. J. Munk, and K. Obermayer, "Analyzing Short-Term Noise Dependencies of Spike-Counts in Macaque Prefrontal Cortex Using Copulas and the Flashlight Transformation," *PLOS Computational Biology*, vol. 5, no. 11, p. e1000577, Nov. 2009.

[23] C. Schlzel and P. Friederichs, "Multivariate non-normally distributed random variables in climate research introduction to the copula approach," *Nonlin. Processes Geophys.*, vol. 15, no. 5, pp. 761–772, Oct. 2008.

[24] G. Papaefthymiou and D. Kurowicka, "Using copulas for modeling stochastic dependence in power system uncertainty analysis," *IEEE Transactions on Power Systems*, vol. 24, no. 1, pp. 40–49, 2009.

[25] W. Li, IEEE Press, and John Wiley & Sons, *Risk assessment of power systems: models, methods, and applications*. Piscataway, NJ; Hoboken: IEEE Press ; John Wiley & Sons . Inc., 2014.

[26] M. J. Eppstein, J. L. Payne, B. C. White, and J. H. Moore, "Genomic mining for complex disease traits with "Random Chemistry"," *Genetic Programming and Evolvable Machines*, vol. 8, no. 4, pp. 395–411, Dec. 2007.

[27] M. J. Eppstein and P. D. H. Hines, "A "Random Chemistry"; Algorithm for Identifying Collections of Multiple Contingencies That Initiate Cascading Failure," *IEEE Transactions on Power Systems*, vol. 27, no. 3, pp. 1698–1705, Aug. 2012.

[28] R. D. Zimmerman, C. E. Murillo-Sanchez, and R. J. Thomas, "MATPOWER: Steady-State Operations, Planning, and Analysis Tools for Power Systems Research and Education," *IEEE Transactions on Power Systems*, vol. 26, no. 1, pp. 12–19, Feb. 2011.

[29] P. Hines and P. Rezaei, *Smart Grid Handbook*. John Wiley & Sons, 2016, ch. Cascading Failures in Power Systems.

[30] R. B. Nelsen, *An introduction to copulas*. New York: Springer, 2010.

[31] L. F. Shampine, "Vectorized adaptive quadrature in MATLAB," *Journal of Computational and Applied Mathematics*, vol. 211, no. 2, pp. 131–140, Feb. 2008.

[32] R. T. Force, "The ieee reliability test system-1996," *IEEE Trans. Power Syst*, vol. 14, no. 3, pp. 1010–1020, 1999.

[33] A. B. Birchfield, T. Xu, K. M. Gegner, K. S. Shetye, and T. J. Overbye, "Grid structural characteristics as validation criteria for synthetic networks," *IEEE Transactions on power systems*, vol. 32, no. 4, pp. 3258–3265, 2017.